Available online at www.sciencedirect.com
ScienceDirect
Catalysis Today 130 (2008) 501–508
CATALYSIS TODAY
www.elsevier.com/locate/cattod

Role of pore size analysis in development of zeolite reforming catalyst

Manoj Kumar, A.K. Saxena, B.S. Negi, N. Viswanadham *

Catalysis and Conversion Process Division, Indian Institute of Petroleum, Dehradun 248005, India

Available online 19 November 2007

Abstract

Effect of preparation variables on the aromatization activity of Pt/KL catalysts was studied. The aromatic content as well as C_5^+ liquid yields were greatly influenced by the nature of binder material used in catalyst preparation. Detailed characterization of the catalysts indicated that two factors, namely (1) nature of binder and (2) size and volume of pores, influenced the catalytic activity. Among the catalysts studied the one prepared by MgO doped basic binder exhibited better performance. Pt loading was also observed to influence the pore volume and aromatization activity of the catalysts, where the catalyst exhibited decrease in pore volume above 0.4 wt.% Pt loading.

Keywords: KL-zeolite; Pore size distribution; Hysterises loop; *t*-plot; Pt dispersion

1. Introduction

Dehydrocyclization of C_6–C_8 paraffins is one of the industrially important options for the value addition of light hydrocarbon containing feed stocks such as light naphtha (LN) and natural gas liquid (NGL) [1,2]. The Pt/KL catalyst is well known for its activity towards the aromatization of such feedstock [3,4]. The exceptionally high activity of the catalyst is ascribed to the optimum pore size of the L-zeolite that can facilitate the ring closure of straight chain hydrocarbon molecule in combination with the dehydrogenation activity of Pt metal to form aromatics [5,6]. However, the narrow channels of L-zeolite are sensitive to the pore blockage by the formation of bigger Pt particles that restrict the product selectivity and catalytic activity [7]. Moreover, the decrease in catalytic activity of Pt/KL was also observed with increasing size of Pt particles [8,9]. Hence, highly dispersed state of Pt metal and its stability against the agglomeration of bigger particles is required to achieve the active catalyst, where, the nature of support also plays an important role [10–15].

Nature and properties of binder materials are also important as they are widely used in the manufacturing of commercial catalysts to improve the mechanical strength. The physico-chemical properties such as pore volume, nature of the binder used in support can influence the metal–support interaction that inturn govern the particle size and agglomeration of Pt. The studies of Jacobs et al. also indicated that the Pt loading by VPI method is efficient on powdered KL but not on the extrudates [16]. That means the efficiency of the vapor phase impregnation is decreased in presence of the binder material in the extrudates. Moreover, incipient wetness impregnation (IWI) is the simple and practical method for the commercial manufacture of reforming catalyst. Our studies on reforming catalysts indicated the importance of pore volume and pore size distribution on the activity of the catalyst [17]. The studies on Pt/mordenite based catalysts also indicated the role of porosity on product yields especially on the selectivity of di-branch isomers [18].

These observations prompted us to study the effect of porosity and nature of binder material on the physico-chemical properties and aromatization activity of Pt/KL catalyst, where, three types of binders, namely, acidic, basic and neutral were used for making three catalysts. All the catalysts were studied for their activity towards light naphtha aromatization reaction.

2. Experimental

2.1. Catalyst preparation

Twenty five grams of Mg30 alumina hydrate (Condea Chemie, Germany) was mixed with 75 g KL-zeolite (Zeolite

* Corresponding author.
E-mail addresses: nvish@iip.res.in, nviswanadham@india.com (N. Viswanadham).

0920-5861/$ – see front matter © 2007 Elsevier B.V. All rights reserved.
doi:10.1016/j.cattod.2007.10.004

Inc., USA) in pastel mortar (on anhydrous basis) and the mixture was peptized thoroughly with 3 vol.% of glacial acetic acid to obtain wet paste The material was shaped to 1.5 mm diameter extrudates by wet extrusion and allowed for drying at room temperature over night, followed by drying at 110 °C for 16 h in oven. The extrudates are then calcined at 500 °C in a muffle furnace for 4 h. The resultant material (basic binder + KL) is named BKL and was used as support for the preparation of Pt catalysts. Incipient wetness impregnation method is used for the Pt loading by using solution of $Pt(NH_4)_4Cl_2$ to give the desired Pt concentration. Three samples namely, BKL-0.4, BKL-0.8 and BKL-1.0 were obtained by loading of 0.4, 0.8 and 1.0 wt.% of Pt, respectively, on the extrudates. The Pt/BKL samples were dried and calcined before using them for characterization and evaluation studies.

The sample AKL-0.4 was obtained by extruding the peptized wet mixture of 25 g acidic alumina (Condea Chemie) and 75 g KL-zeolite (Zeolite Inc.), following the similar procedure of drying and Pt loading mentioned as in BKL-0.4. The sample obtained with acidic binder is denoted as AKL-0.4. Similarly, the sample prepared using silica sol as binder was denoted as SKL-0.4.

2.2. Physico-chemical characterization

Surface area and pore size distribution of samples were determined volumetrically by physisorption of nitrogen at liquid nitrogen temperature (77 K) in static mode using ASAP–2010 Micromeritics (USA) instrument. For measuring surface area, 0.2010 g of sample is taken in a specially designed sample tube and degassed at 300 °C under vacuum of 10^{-3} Torr for 4 h. A frit is attached to the mouth of the sample tube, so that when the sample tube is removed from preparation mode, it does not allow sample to expose in atmosphere. Sample is cooled to room temperature under vacuum and the sample tube is removed from preparation port and attached to analysis port of the instrument. For all the samples, N_2 adsorption–desorption isotherms were obtained at 77 K and the temperature was maintained constant by using liquid nitrogen, whereas helium gas was used for measuring dead space. Surface area, pore volume and pore size distribution were obtained by measuring volume adsorbed at different P/P_0 values and by applying different methods. Total pore volume was estimated by measuring the volume of gas adsorbed at P/P_0 of 0.998, whereas, *t*-plot method was used to calculate the micropore surface area (<20 Å) using Harkins–Jura equation. The volume distribution in mesopores was obtained from the adsorption branch of the isotherm by applying BJH method. Total micropore volumes (<20 Å) of the samples were obtained using Horvath–Kawazoe method [19].

The dispersion of Pt was measured by carrying out oxygen titration using a dynamic pulse flow technique (Pulse Chemisorb 2700, Micromeritics). The details of the method have been described elsewhere [20]. The catalyst (1 g) after pretreatment at 500 °C for 2 h in the flow of helium carrier gas was reduced at 500 °C for 3 h in hydrogen flow (50 cm^3/min) and was then cooled to room temperature (RT) in the flow of hydrogen and flushed with carrier gas. The first oxygen titration (OT1) was then carried out at RT. The catalyst after OT1 was treated with hydrogen gas at RT for half an hour, flushed with helium and then second oxygen titration OT2 was conducted. The Pt dispersion was determined from OT2.

Microcalorimetric studies of adsorption of ammonia have been performed to determine total acidity and acid strength distribution using a Tian–Calvet type heat flux microcalorimeter (Model C-80 Setaram, France) connected to a volumetric adsorption unit for sample treatment and probe molecule delivery. Samples were preheated at 450 °C under vacuum for 4 h prior to microcalorimetric measurements. The heats evolved from sequential doses of ammonia onto the sample were measured at 175 °C. The heat of adsorption generated for each dose was calculated from the resulting thermo grams and the amount of ammonia adsorbed from the pressure change. Sequential doses give the differential heat of NH_3 adsorption as a function of coverage (i.e., differential heat curves). It provides the information about the number and strength of acid sites on samples.

2.3. Catalyst evaluation

Light naphtha containing C_5, C_6 paraffins and naphthenes was used for the activity studies. The component wise analysis of the hydrocarbon types in the light naphtha feed is given in Table 1.

The light naphtha aromatization reaction was carried out in a high-pressure micro reactor unit. All the catalysts were reduced in presence of hydrogen at 520 °C for 6 h, prior to the reaction. Reactant was fed at a WHSV of 2 h^{-1} at hydrogen-to-hydrocarbon molar ratio of 5. All experiments were carried out at 460 °C, 6 bar pressure. The reaction product was analyzed using Hewlett Packard gas chromatograph model 5730 A, fitted with a TCEP column and FID detector. Gaseous products were analyzed using a Squalane column. The conversion and selectivity of the products were calculated based on the formulae given below

$$\text{Selectivity}\,(\%) = \frac{\text{weight of the product component}}{\text{weight of the total product}} \times 100$$

Table 1
Light naphtha feed composition

Hydrocarbon types	*n*-Paraffins	Iso-paraffins	Naphthenes	Aromatics
Pentane	0.4	–	0.9	–
Hexane	16.2	13.7	19.3	21.3
Heptane	4.2	10.3	4.3	1.1
Octane	–	5.8	1.5	–
Nonane	–	1.0	–	–
Total	20.8	30.8	26.0	22.4

3. Results and discussion

3.1. Effect of Pt amount on pore volume and pore size distribution

Nitrogen adsorption–desorption isotherms of BKL support and three Pt loaded BKL samples are given in Fig. 1. The shapes of the curves indicate the type-IV isotherm according IUPAC nomenclature which is a characteristic of mesoporous materials [21]. According to the same classification, the shapes of the hysteresis loops were further classified into four types, where the samples of the present study exhibited type H3 hysteresis loops. These types of hysteresis are usually formed by aggregates or agglomerates of particles forming slit shaped pores (plates or edged particles like cubes). The shape of the hysteresis loop is similar for all the samples, except the area of the loops. The area is almost similar for the BKL support and the 0.4 wt.% Pt loaded BKL (BKL-0.4). But, it is decreased a little in case of samples prepared by higher metal loadings, namely, 0.8 wt.% Pt (BKL-0.8) and 1.0 wt.% Pt (BKL-1.0). These results indicate the decrease in pore volume of the samples at higher metal loadings.

The decrease in pore volume can be further observed from the data given in Table 2, where, the total pore volume of KL support (BKL) and three metal loaded samples are 0.22, 0.22, 0.18 and 0.17 cm^3/g, respectively. The micropore volume was also decreased from 0.079 cm^3/g of BKL to ~0.047 cm^3/g for samples BKL-0.8 and BKL-1.0. The data indicate significant decrease (~40%) in pore volume of BKL-0.8 and BKL-1.0. Effect of metal loading on the microporosity (up to 20 Å) of the samples can be understood from the *t*-plots of the samples given in Fig. 2. The intercept indicates the volume in micropores of the samples, where BKL support and BKL-0.4 exhibited almost equal micropore volume (77×10^{-3} cm^3/g). But, the micropore volume is decreased to around 55×10^{-3} cm^3/g for the samples of higher metal loading, namely, BKL-0.8 and BKL-1.0 (at 0.8 and 1.0 wt.% Pt loadings) respectively.

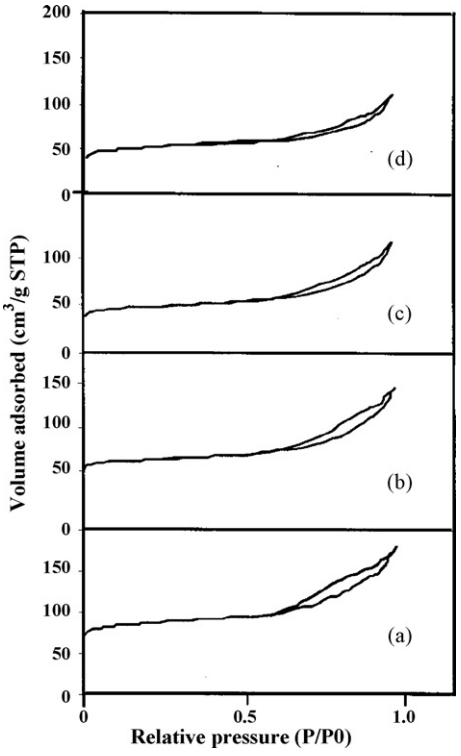

Fig. 1. Adsorption–desorption isotherms of N_2 at 77 K for the samples: (a) BKL, (b) BKL-0.4, (c) BKL-0.8 and (d) BKL-1.0.

The BJH cumulative pore volume curves given in Fig. 3 also indicate the loss in pore volume at higher Pt loadings. The samples KL support and BKL-0.4 exhibited high pore volume in the entire range of pores (up to1750 Å) that cover micropores, mesopores and macropores. The curves indicate that the pore volume is higher in the samples BKL and BKL-0.4. The pore volume is decreased in the samples BKL-0.8 and BKL-1.0 and the lowest value of pore volume was exhibited by sample BKL-1.0. This observation suggests occupation of Pt clusters in the binder as well as KL support of these samples at higher metal loadings. Careful analysis of the curves in Fig. 3 indicates that the decrease in pore volume is more prominent in the micropore region. For comparison, the volume in the entire range of pores is divided into three regions, namely, A–B, B–C, and C–D corresponding to the pores of diameters up to 500, 500–1250 and above 1250 Å, respectively. The curves of BKL support as well as BKL-0.4 are almost super imposed indicating equal pore volume in the all three pore size regions of these samples and no loss is observed in pore volume of the sample after 0.4 wt.% Pt loading. For the sample BKL-0.8, the pore volume decrease was more at A–B region, moderate at B–C region and low at C–D region. Sample BKL-1.0 exhibited further decrease in pore volume in the pore region of A–B, but exhibited similar pore volume with BKL-0.8 in the region of B–C and C–D. Overall, the decrease of volume in pores of various diameters followed the following order: 0–500 Å > 500–1250 Å > above 1250 Å. That means, increase in metal loading affects more volume in micropores and smaller mesopores (up to 500 Å) compared to that of the larger mesopores (>500 Å) and macropores (>1250 Å). The volumes in pores of various diameters have been calculated. Based on these values a pore size distribution histogram is made in Fig. 4. The histogram suggests that there is no remarkable change in the pore volume of the support at the Pt loading of 0.4 wt.% (BKL-0.4). However, the pore volume was decreased above the Pt level of 0.4 wt.%, i.e., BKL-0.8 and BKL-1.0. The decrease in micropore volume (<10 Å) observed only at the high Pt loadings. There was a slight decrease in the volume of the mesopores also. Among the pores of various diameters, the volume in mesopores of >500 Å was decreased significantly followed by a small decrease in micropores of <10 Å. The volume in pores of diameter 10–500 Å is changed in negligible amounts. That means Pt agglomeration is affecting the mesopores of (>500 Å) binder as well as the micropores of the KL-zeolite.

All these results suggest the pore volume decrease of the KL support at the Pt loadings of above 0.4 wt.%. This is in agreement with the studies of Jacobs et al. where, the agglomeration of Pt was observed in the sample prepared by loading 1 wt.% Pt [16]. But Jacobs et al. did not study the

Table 2
Physico-chemical characterization and aromatization performance of Pt loaded KL based catalysts

Sample	BKL	BKL-1.0	BKL-0.8	BKL-0.4	AKL-0.4	SKL-0.4
Pt loading (wt.%)	0.0	1.0	0.8	0.4	0.4	0.4
Surface area, pore size distribution and Pt dispersion by sorption						
BET surface area (m^2/g)	250	179	187	239	292	122
External surface area (m^2/g)	45	73	59	44	112	41
Micropore area (m^2/g)	198	114	120	195	179	81
Total pore volume (cm^3/g)	0.22	0.17	0.18	0.22	0.40	0.11
Micropore volume (cm^3/g)	0.079	0.047	0.049	0.078	0.073	0.033
Pt dispersion (%)	–	53	55	71	28	51
Acidity and strength distribution by micro calorimetric ammonia adsorption						
Total acidity (mmol/g)	0.29	0.27	0.28	0.29	0.40	0.33
Strong (mmol/g) ($\Delta_{NH_3} > 100$ kJ mol^{-1})	0.06	0.03	0.04	0.05	0.17	0.10
Medium (mmol/g) (Δ_{NH_3} = 100–75 kJ mol^{-1})	0.06	0.06	0.06	0.06	0.08	0.06
Weak (mmol/g) ($\Delta_{NH_3} > 100$ kJ mol^{-1})	0.17	0.18	0.18	0.18	0.15	0.17
Performance in light naphtha aromatization						
Conversion (wt.%)	–	95.0	98.4	100.0	100.0	72.0
Product selectivity (wt.%)						
C_1–C_2	–	2.1	0.9	0.4	8.2	3.8
C_3–C_4	–	2.3	1.5	0.6	7.6	5.6
C_5^+ liquid	–	92.6	94.5	96.0	74.2	88.5
(Aromatics content in C_5^+ liquid)	–	(44.5)	(48.2)	(53.0)	(36.6)	(48.8)
Hydrogen	–	3.0	3.1	3.0	1.0	2.1
Total	–	100.0	100.0	100.0	100.0	100.0

Δ_{NH_3} = heat of adsorption of ammonia on acid sites.
Reaction conditions: feed = light naphtha, reaction temperature = 460 °C, pressure = 6 bar, WHSV = 3 h^{-1} and H_2/HC = 5 (mol/mol).

activity of catalysts at lower metal loadings. Our data on BKL-0.4 differs with that of BKL-1.0 as there is no loss in pore volume occurred at lower metal loadings. This observation suggests the importance of the optimum amount of Pt to be impregnated, where, the BKL-0.4 with 0.4 wt.% Pt exhibited very high Pt dispersion without any loss in pore volume.

The *n*-octane aromatization studies of Jongpatiwut et al. suggested the diffusion constraints of xylenes even in the sample prepared by VPI method when the amount of Pt is 1.0 wt.% [22]. The present study indicates that 0.4 wt.% Pt as the optimum amount to restrict the formation of Pt agglomerates. The Pt dispersion values (Table 2) also suggest the highest dispersion of Pt at 0.4 wt.% loading that may be due to the uniform distribution of Pt particles without agglomeration. The study indicates the importance of metal amount in catalyst preparation. Our earlier studies on rhenium encapsulated ZSM-5 also indicated the importance of rhenium amount on the selective oxidation of propylene [23]. Up to the 4.5 wt.% rhenium loading the strong metal–support interaction facilitated the formation of nano clusters of rhenium oxide active sites. But, the increasing rhenium loading resulted in the formation of weakly adsorbed rhenium oxide species on the ZSM-5 that is converted into the inactive Re_2O_4 species [24].

Literature reports also indicated that the amount of Pt loaded on KL should be optimum for its activity towards catalytic reactions. According to the reports of Treacy et al., there exist an optimum length-loading window of Pt/KL catalysts that can be expressed as $0.25 \leq wl \leq 0.5$, where, w is the percentage of

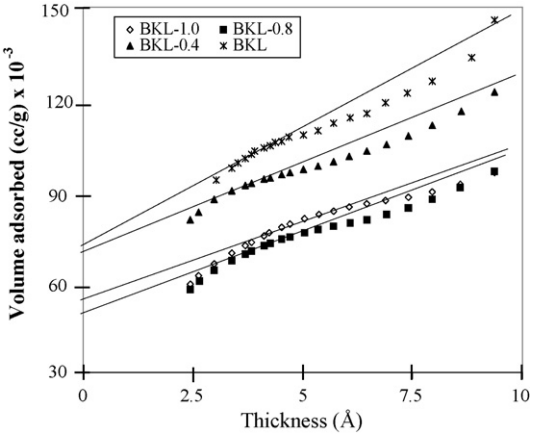

Fig. 2. *t*-plots of the Pt/KL samples.

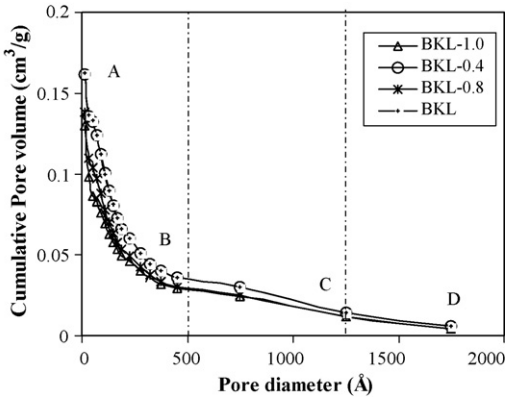

Fig. 3. BJH adsorption cumulative pore volume plots of the samples.

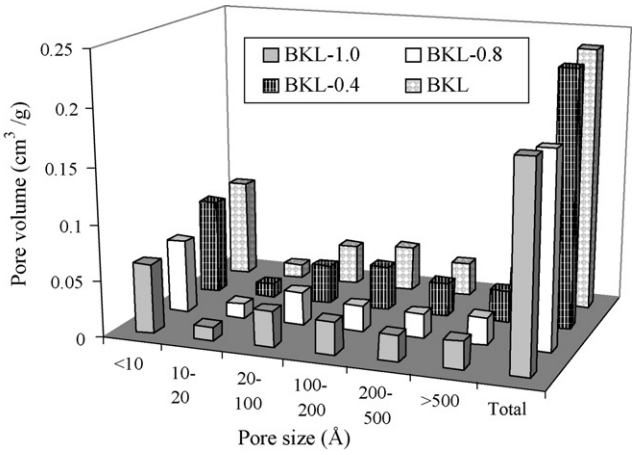

Fig. 4. Pore size distribution.

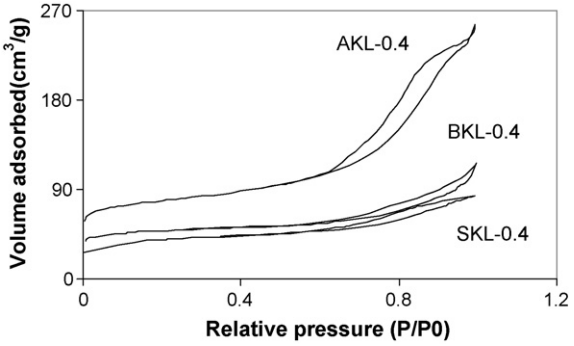

Fig. 5. Effect of binder material on the adsorption–desorption isotherms Pt/KL samples.

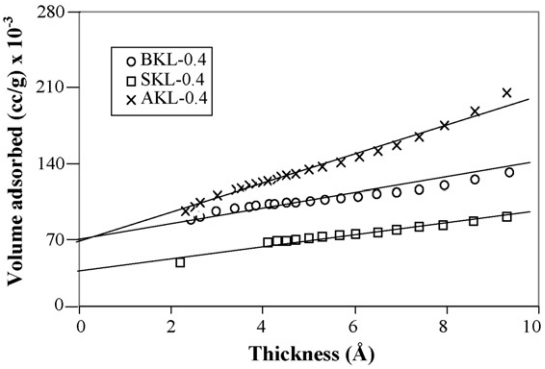

Fig. 6. Effect of binder material on *t*-plot patterns of the Pt/KL samples.

Pt by weight in the zeolite, and l is the channel length (μm) [10]. Thus, for an L-zeolite of 1 μm, the weight of the Pt loading should be in the range of 0.25–0.5. However, studies of McVicker et al. indicated that at 0.6 wt.% Pt loading, the catalyst exhibited a good correlation with the benzene yield and the Pt dispersion in *n*-hexane conversion [10,25]. Results of the present study indicated that the catalyst exhibited the best catalytic activity at 0.4 wt.% Pt loading. The pore volume results obtained for BKL of the present study also indicated the 0.4 wt.% (BKL-0.4) of Pt as the optimum metal loading for avoiding the loss of pore volume. This observation supports the optimum metal loading theory of Treacy et al. [7].

Overall, the studies on Pt loaded KL samples indicated that 0.4 wt.% Pt as the optimum amount for retaining the porosity properties of KL support. The studies also indicate the role of mesoporosity in the distribution of Pt metal. The porosity and the nature of binder may influence the formation of Pt particles in the mesopores. In order to see this aspect, three samples prepared by using three different types of binder materials, namely, acidic alumina (AKL-0.4), basic alumina (BKL-0.4) and silica sol (SKL-0.4) were studied. All the samples have similar amount of binder and Pt metal loading (0.4 wt.%).

3.2. Effect of binder material on pore volume and pore size distribution

The nitrogen adsorption–desorption isotherms of the three samples prepared by mixing three types of binder materials to the KL, namely, basic binder to KL (BKL), acidic binder to KL (AKL) and silica sol to KL (SKL) are given in Fig. 5. All the three samples exhibited the type-IV of isotherm. The hysteresis loops indicated the presence of mesoporosity and the volume of the loops indicate the mesoporosity in the order of AKL > BKL > SKL. The slope of the curves up to 0.05 P/P_0 relative pressure indicate the filling of micropores, where, the order of micropore volume was observed to be similar to that of mesopore volume. The micropore volume of the samples obtained from *t*-plot method (Fig. 6) also indicated the decrease in micropore volume in the similar order; AKL > BKL > SKL. That means the volume in both meso and micropores is lower in case of basic binder and silica sol binder samples. The BJH cumulative pore volume plot in Fig. 7 clearly indicates the differences in the volume of pores in the entire range of pore diameter. The sample AKL exhibited very high pore volume up to the pore diameter of 300 Å. Above the pore diameter of 300 Å, the samples AKL and BKL exhibited similar pore volume patterns. However, sample SKL exhibited lower pore volume in the entire range of pore diameter studied.

Differences in mesopore volumes of the three samples can be explained on the basis of difference in the porosity of the three different binder materials used in their preparation. But, the difference in the micropore volume of the samples cannot be explained by the same reason. Since all the samples have

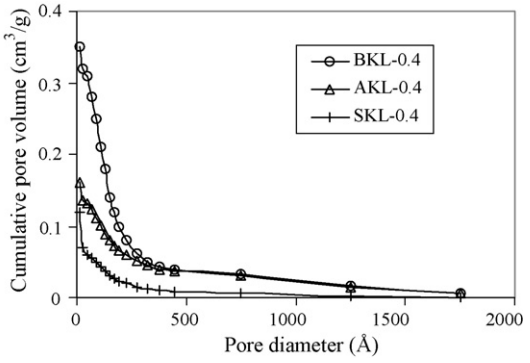

Fig. 7. Effect of binder material on BJH adsorption cumulative pore volume plots of Pt/KL samples.

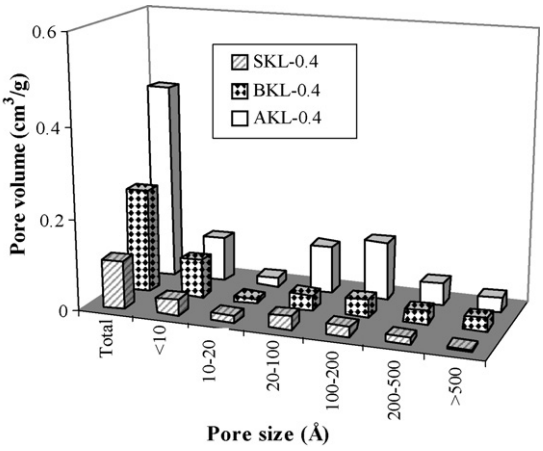

Fig. 8. Effect of binder material on the overall pore size distribution of Pt/KL samples.

similar amount of KL-zeolite and Pt amount, the micropore volume representing the zeolitic pores (<10 Å) should theoretically be same. In order to explain this aspect, the volumes in micropores (zeolite) as well as the entire range of mesopores is plotted in a histogram (Fig. 8). The pore volume in micropores of <10 Å is similar for AKL-0.4 and BKL-0.4 samples but is lower in case of SKL-0.4 sample. That means, the zeolite pore volume in SKL-0.4 is decreased even at lower (0.4 wt.%) Pt loading. This behavior of SKL-0.4 is different from that of BKL-0.4 thus suggests the importance of nature of binder on the preferential occupation of Pt in the KL-zeolite based catalysts. Absence of wider mesopores and macropores in the SKL may be the reason for the decrease in micropore volume by Pt occupation in this sample. The Pt dispersion values followed the same trend of mesoporosity i.e., AKL > BKL > SKL.

3.3. Performances of catalysts in light naphtha aromatization reaction

The performances of catalysts in light naphtha aromatization are given in Table 2. The products obtained were classified into four groups, namely (1) fuel gas ($C_1 + C_2$), (2) LPG ($C_3 + C_4$), (3) C_5^+ liquid and (4) hydrogen. Among these, C_5^+ liquid and hydrogen are considered desired products, and fuel gas and LPG are considered undesired products that are usually formed due to cracking activity of the catalyst.

The data obtained on BKL-0.4, BKL-0.8 and BKL-1.0 indicates the effect of metal amount on aromatization performance of the BKL. All the catalysts exhibited considerable aromatization activity and hydrogen production. Among the three catalysts, the BKL-0.4 exhibited best performance in terms of conversion and C_5^+ selectivities. The selectivity towards fuel gas and LPG was also low on this catalyst. This catalyst also exhibited no loss in pore volume after Pt loading indicating the presence of homogenously distributed Pt in BKL-0.4 catalyst. The Pt dispersion measurements also support the well-dispersed Pt in BKL-0.4. These properties of the BKL-0.4 may be responsible for its high aromatization activity and low cracking activity.

In order to see the effect of porosity and nature of the binder, the aromatization performance of basic binder containing catalyst BKL-0.4 was compared with those prepared using acidic alumina (AKL-0.4) and silica sol binders (SKL-0.4). As from the data given in Table 2, BKL-0.4 exhibited best aromatization performance among the three catalysts. In spite of high mesoporosity and microporosity, the sample AKL-0.4 exhibited lower aromatic yields compared to the BKL-0.4. As the acidic supports are known to affect the interaction of Pt and the electron density on Pt, the lower dehydrogenation activity of the Pt supported on acidic support in AKL-0.4 may be responsible for its lower aromatization activity. The higher selectivity towards fuel gas and LPG exhibited by AKL-0.4 may be due to the undesired cracking reactions prevailed on the acidic support. The micro calorimetric acidity values of the samples indeed confirmed the presence of more strong acid sites in sample AKL-0.4.

Catalyst SKL-0.4 exhibited lower conversion among all the five catalysts. The product selectivity of C_5^+ and aromatics on SKL-0.4 are in between to those of the BKL-0.4 and AKL-0.4. Overall, the aromatization activity of three binder supported catalysts followed the basic nature of the support i.e., BKL-0.4 > SKL-0.4 > AKL-0.4.

3.4. Factors responsible for activity of BKL-0.4

Overall, the nature of binder and Pt amount influenced the pore volume and aromatization activity of Pt/KL catalyst. It is known that strong metal–support interaction can modify both electronic state and particle size of the metal in the supported catalyst, where acidic nature of support attracts electrons from the metal [13,16–18]. Studies of Arcoya et al. also revealed the importance of the electron density on the Pt and its dependence on the acidity of the support [26,27]. The residual acidity on Pt exchanged samples decreased the electron density on Pt particles and thus decreased its dehydrogenation activity. Similar type of phenomenon is also reported for Mo loaded MgO–Al_2O_3 mixed oxide supports used for hydro-desulphurization reactions. The studies indicated the importance of the nature of support on metal–support interaction [28]. The electro negativity of metal ions of oxides varies in the following order MgO < Al_2O_3 < TiO_2 < SiO_2. Larger the electro negativity stronger is the metal–oxygen bond of the support. In other words, with decrease in electro negativity, metal–oxygen interaction in the support becomes weaker, and hence, the coordination ability of lattice oxygen increases. As electro negativity of Mg ions is the lowest among the metal ions of other oxides studied thus the coordination ability of oxygen atom of MgO in the support is the highest for metal loaded. Based on this theory, the BKL support (KL + Mg doped alumina binder) having MgO can exhibit better interaction with the Pt atoms that can discourage the Pt–Pt interaction and the formation of Pt agglomerates responsible for loss of pore volume in the catalyst BKL-0.4. Similarly, the decrease in electron density on Pt caused by the acidic binder in the support of AKL-0.4 may be responsible for its lower aromatization activity. The lower microporosity observed in SKL-0.4 after Pt

loading, resulted in lowest aromatic yields and conversions on this sample. The decrease in pore volume of the samples AKL and SKL can also indicate the formation of Pt agglomerates in the same order. Among the three types of binders used, the BKL could exhibit best catalytic activity when 0.4 wt.% of Pt is loaded. The optimum amount of Pt and its dispersion vary with the nature of binder material. The basic nature of the binder and the absence of any acid sites in the BKL along with the considerable amount of micropore and mesopore volume could exhibit the highest aromatic yield among the three samples.

Overall, the results indicated that the performance of catalysts affected by the change in porosity caused by acidity or basicity of the support that govern the preferential metal–support interaction and Pt agglomeration on the support. This will greatly influence the pore volume patterns and the aromatization activity of the catalysts. The studies indicate that the nature of binder material as well as the amount of Pt metal loaded on the KL support can influence the metal–support interaction. Though the nature of support and metal amount are seem to be two different factors yet related with a common phenomenon of metal–support interaction that is responsible for observed changes in pore size distribution and aromatization activity of the catalysts. Among the binders, the basic nature of binder facilitated the strong metal–support interaction. Similarly, the metal–support interaction is efficient at the low metal loadings. Strong metal–support interactions can discourage the affinity of Pt particles to interact with other metal particles i.e., metal–metal interaction decreases. Similarly, the weak metal–support interaction can encourage the metal–metal interaction that results in agglomeration or growth of Pt particles.

The role of metal–support interaction on the catalytic properties can be explained from the schematic depicted in Fig. 9, where the Pt loading on two supports, namely, (a) KL + basic binder and (b) KL + acidic binder is given. Case 1 and 2 of the Fig. 9 represent the effect of Pt amount on basic binder containing KL support and case 3 on the acidic binder containing support. In case 1, the low Pt loading (0.4 wt.%) can lead to the mono-layer type adsorption of Pt atom on the support, that can facilitate a strong metal–support interaction (SMSI). The stronger the metal–support interaction, the weaker will be the metal–metal interaction. This can be explained in terms of electron density on the Pt atoms, where, the high electron density on Pt is known to have lesser tendency to the formation of particles or agglomerates due to the repulsion of the electrons on the nearby Pt. The strong interaction of Pt with the support such as basic KL can stabilize the electron density on Pt. The high electron density on Pt stabilized by the basic binder and basic KL in BKL support can discourage the metal–metal interaction and the formation of Pt agglomerates that are

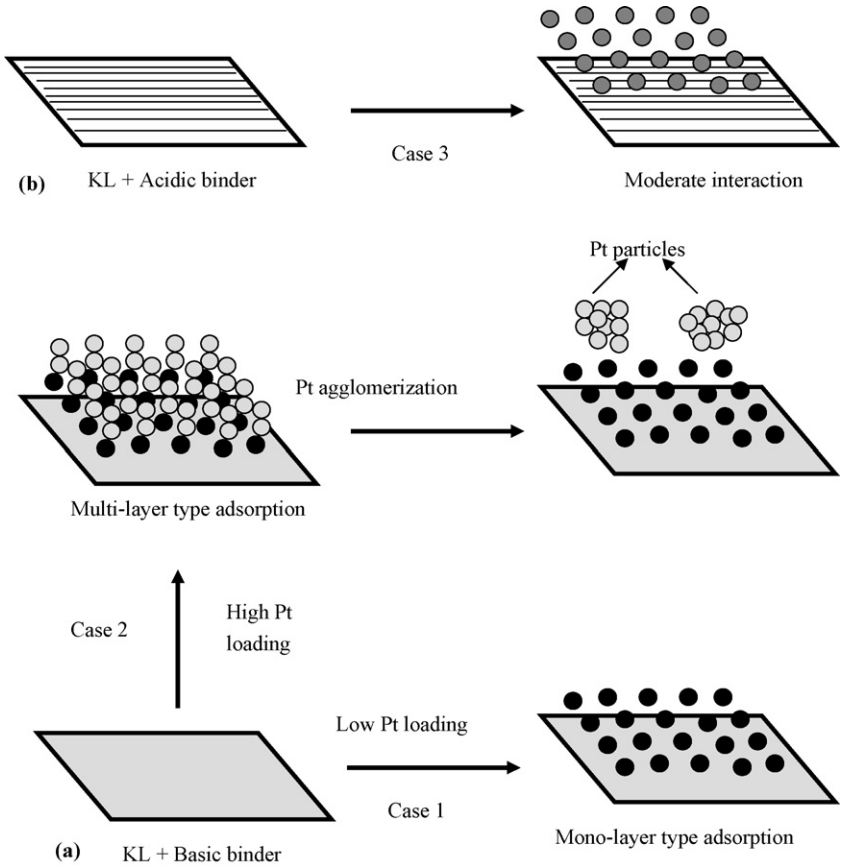

Fig. 9. Schematic view of possible Pt–support interactions at: (case 1) basic binder and lower Pt amount, (case 2) basic binder and higher Pt amount and (case 3) acidic binder and lower Pt amount. (●) Pt sites located near to the surface of basic support having strong interaction. (◯) Pt sites located away from the surface of basic support having weak interaction. (◯) Pt sites on the acidic support having moderate interaction.

otherwise can cause the loss of pore volume and catalytic activity. The pore volume and pore size distribution studies indeed indicated that there is no loss of volume in pores of all the diameter range present in KL as well as binder in the sample BKL-0.4. The Pt dispersion was also high for this sample that supports the homogenously distributed Pt in BKL-0.4. This is an ideal situation to prevent the agglomeration of Pt and the pore volume loss of the catalyst that is responsible for the high aromatization selectivity of BKL-0.4 in the present study.

Case 2 in Fig. 9 represents the situation where the amount of Pt loaded is high (viz. 1.0 wt.%). At this situation, the excess amount of Pt available can exhibit a multi-layer type of adsorption on the support, where, the Pt atoms in the first layer can have strong interaction with the support, while the rest of the Pt located in other sub layers (away from the support) can exhibit relatively weaker interaction with the support. This is a situation where the Pt atoms located in different layers can behave in a different way due to the variation in strength of interaction with support and resultant variation in electron density on Pt. The Pt atoms having weaker interaction with the support can show strong tendency to interact with the nearby Pt that leads to the formation of Pt agglomerates. This phenomenon explains why the pore volume decrease was observed in BKL-0.8 and BKL-1.0 catalyst. The lower activity of Pt located in agglomerates and its occupation in narrow channels of zeolite also affects the catalyst performance. In spite of high Pt amount, the low pore volume and aromatization activity exhibited by BKL-1.0 when compared to BKL-0.4 clearly supports this phenomenon of heterogeneous metal–support interaction.

Case 3 in Fig. 9 represents the situation, where the support containing acidic binder. The metal loading on such support can exhibit relatively lower metal–support interaction due to the decrease in electron density on Pt caused by acidic binder in the support. Such catalyst is expected to exhibit poor catalytic properties even at lower Pt loadings (AKL-0.4). In spite of high mesoporosity, the low Pt dispersion and aromatization activity exhibited by AKL-0.4 clearly supports the phenomenon of weak metal–support interaction.

Based on these studies, we believe that the better catalytic properties exhibited by BKL-0.4 is due to the better metal–support interaction facilitated by the basic nature of binder as well as the low amount of Pt loaded on this catalyst. The optimum amount of Pt may depend on volume in pores of KL, volume in pores of the binder and the basic nature of the binder. By taking care of these aspects, an active aromatization catalyst can be prepared by IWI method which is suitable for catalyst scale up and industrial applications.

4. Conclusions

Nature of binder and Pt loadings played an important role in catalytic properties and aromatization activity of the Pt/KL reforming catalyst. The BKL-0.4 catalyst prepared by 0.4 wt.% of Pt loaded on the basic binder containing KL support exhibited better catalytic properties such as no loss in pore volume and surface area after metal loading. Above 0.4 wt.% Pt loadings, the catalyst exhibited decrease in pore volume and percent dispersion of Pt indicating the Pt agglomeration above the 0.4 wt.% loading in the zeolite pores. In spite of high mesoporosity, the sample prepared using acidic alumina binder (AKL-0.4) could not yield better aromatization activity. The catalyst prepared using silica sol binder (SKL-0.4) also exhibited poor catalytic properties due to the narrow range pores. The studies indicated that IWI method can be used for the preparation of active and stable catalysts for aromatization by following the principle of optimum metal loading, where pore volume analysis can provide valuable information.

Acknowledgements

Our sincere thanks to the Director, Indian Institute of Petroleum, for his kind suggestions and encouragement. Our thanks to the Zeolite Inc., US for supplying the L-zeolite.

References

[1] N. Viswanadham, G. Murali Dhar, T.S.R. Prasada Rao, J. Mol. Catal. A 125 (1997) L87.
[2] N. Viswanadham, J.K. Gupta, L. Dixit, M.O. Garg, J. Mol. Catal. 258 (2006) 15.
[3] T.R. Hughes, W.C. Buss, P.W. Tamm, R.L. Jacobson, Stud. Surf. Sci. Catal. 28 (1986) 725.
[4] G. Jacobs, C.L. Padro, D.E. Resasco, J. Catal. 179 (1998) 43.
[5] E.G. Derouane, D.J. Vanderveken, Appl. Catal. 45 (1988) L15.
[6] S.T. Tauster, J.J. Steger, J. Catal. 125 (1990) 387.
[7] M.M.J. Treacy, Micropor. Mesopor. Mater. 28 (1999) 271.
[8] J. Zheng, J.L. Dong, Q.H. Xu, Stud. Surf. Sci. Catal. 84 (1994) 1641.
[9] F.J. Maldonado, T. Becue, J.M. Siva, M.F. Ribeiro, P. Massiani, M. Kermarec, J. Catal. 195 (2000) 342.
[10] W.M.H. Sachlter, Catal. Today 15 (1992) 419.
[11] T. Schmauke, M. Menzel, E. Roduner, J. Mol. Catal. 194 (2003) 211.
[12] J. Zheng, T. Schmauke, E. Roduner, J.L. Dong, Q.H. Xu, J. Mol. Catal. 171 (2001) 181.
[13] F.J. Maldonado, T. Bécue, J.M. Siva, M.F. Ribeiro, P. Massiani, M. Kermarec, J. Catal. 195 (2000) 342, and references there in.
[14] C. Besoukhanova, J. Guldot, D. Bearthomeuf, M. Breysse, J.R. Bernard, J. Chem. Soc. Faraday Trans. 77 (1981) 1595.
[15] G. Larsen, G.L. Haller, Catal. Lett. 3 (1989) 103.
[16] G. Jacobs, W.E. Alvarez, D.E. Resasco, Appl. Catal. 206 (2001) 267.
[17] L.D. Sharma, M. Kumar, A.K. Saxena, M. Chand, J.K. Gupta, J. Mol. Catal. 185 (2002) 135.
[18] N. Viswanadham, M. Kumar, Micropor. Mesopor. Mater. 92 (2006) 31.
[19] J. Schmidt, A. Boisen, E. Gustavssion, K. Stahl, S. Pehrson, S. Dahl, A. Carlsson, C.J.H. Jacobsen, Chem. Mater. 13 (2001) 4416.
[20] L.D. Sharma, M. Kumar, A.K. Saxena, D.S. Rawat, T.S.R. Prasada Rao, Appl. Catal. A 168 (1998) 251.
[21] A.E. Persson, B.J. Schoeman, J. Sterte, J.E. Otterstedt, Zeolites 14 (1994) 314.
[22] S. Jongpatiwut, P. Sackamduang, T. Rirksomboon, S. Osuwan, D.E. Resasco, J. Mol. Catal. 218 (2003) 1.
[23] N. Viswanadham, T. Shido, Y. Iwasawa, Appl. Catal. A: Gen. 219 (2001) 223.
[24] N. Viswanadham, Takafumi Shido, Takehiko Sasaki, Y. Iwasawa, J. Phys. Chem. B 106 (2002) 10955.
[25] G.B. McVicker, J.L. Kao, J.J. Zeimiak, W.E. Gates, J.L. Robbins, M.M.J. Tracy, S.B. Rice, T.H. Vanderspurt, V.R. Cross, A.K. Ghosh, J. Catal. 39 (1993) 48.
[26] A. Arcoya, X.L. Seoane, J.M. Grau, Appl. Surf. Sci. 205 (2003) 206.
[27] A. Arcoya, X.L. Seoane, J.M. Grau, Appl. Catal. 284 (2005) 85.
[28] M. Kumar, F. Aberuagba, J.K. Gupta, K.S. Rawat, L.D. Sharma, G. Murali Dhar, J. Mol. Catal. A 213 (2004) 217.